Talanta 117 (2013) 543–548

Contents lists available at ScienceDirect

Talanta

journal homepage: www.elsevier.com/locate/talanta

Short communication

Optimization of a hydride generation metallic furnace atomic absorption spectrometry (HG-MF-AAS) method for tin determination: Analytical and morphological parameters of a metallic atomizer

Rodrigo Moretto Galazzi [a,b], Marco Aurélio Zezzi Arruda [a,b,*]

[a] Department of Analytical Chemistry, Group of Spectrometry, Sample Preparation and Mechanization—GEPAM, Institute of Chemistry, University of Campinas—UNICAMP, P.O. Box 6154, 13083-970 Campinas, SP, Brazil
[b] National Institute of Science and Technology for Bioanalytics, Institute of Chemistry, University of Campinas—UNICAMP, P.O. Box 6154, 13083-970 Campinas, SP, Brazil

ARTICLE INFO

Article history:
Received 24 July 2013
Received in revised form
13 September 2013
Accepted 18 September 2013
Available online 25 September 2013

Keywords:
Hydride generation
AAS
Metallic furnace
Sn

ABSTRACT

The present work describes a metallic tube as hydride atomizer for atomic absorption spectrometry. Its performance is evaluated through tin determination, and the accuracy of the method assessed through the analysis of sediment and water samples. Some chemical parameters (referring to the generation of the hydride) such as acid, NaOH and THB concentrations, as well as physical parameters (referring to the transport of the hydride) such as carrier, acetylene, air flow-rates, flame composition, coil length, tube hole area, among others, are evaluated for optimization of the method. Scanning electron microscopy is used for evaluating morphological parameters in both new and used (after 150 h) tube atomizers. The method presents linear Sn concentration from 50 to 1000 $\mu g\,L^{-1}$ ($r > 0.9995$; $n = 3$) and the analytical frequency of ca. 40 h^{-1}. The limit of detection (LOD) is 7.1 $\mu g\,L^{-1}$ and the precision, expressed as RSD is less than 4% (200 $\mu g\,L^{-1}$; $n = 10$). The accuracy is evaluated through reference materials, and the results are similar at 95% confidence level according to the *t*-test.

1. Introduction

The hydride generation metallic furnace atomic absorption spectrometry (HG-MF-AAS) using a ceramic capillary for introducing gaseous samples (as hydrides) into the atomizer was recently proposed [1], and it can be considered a variant mode of the thermospray flame furnace atomic absorption spectrometry (TS-FF-AAS), proposed by Gáspár and Berndt [2]. This technique allies the advantages for working with microflames (as MMQTA [3] or their own TS-FF-AAS [2]) as well as the different reaction environment when compared with quartz tubes for hydride generation [1]. Another advantage is that similar devices used for hydride generation with quartz tubes can also be employed when HG-MF-AAS is applied. Additionally, the low cost of this technique can be another factor for its implementation to any laboratory.

The HG-MF-AAS was already proposed for a diversity of analytes, such as As, Bi, Sb, and Se in their total forms [4–6], and recently for inorganic As speciation [7]. In this last example, mild conditions were attained for hydride generation as well as for extraction, using microwave-assisted extraction (MAE). Another interesting feature is the diversity of samples employed when focusing on HG-MF-AAS. Medicinal, urine, sediment, animal, water, and plankton samples were already used, indicating its good potentiality as analytical technique, as well as the accuracy of the proposed methods.

In view of these advantages, the absence of a method for tin determination using this technique, and the importance and the difficulty in accurately determine this element, the aim of this work was to propose an accurate and reliable method based on HG-MF-AAS technique for tin determination. Chemical and physical parameters were evaluated for optimizing the method, and sediment and water samples were employed for accuracy tests. Additionally, the morphology of the tube atomizer was evaluated along the optimization in order to follow possible changes on the nature of the tube atomizer.

2. Experimental

2.1. Equipments

For all Sn determinations a Perkin-Elmer AAnalyst 300 flame atomic absorption spectrometer (FAAS) equipped with deuterium lamp background correction and PE-AA WinLab software was used. Electrodeless discharge lamp (EDL) as primary radiation

* Corresponding author at: National Institute of Science and Technology for Bioanalytics, Institute of Chemistry, University of Campinas—UNICAMP, P.O. Box 6154, 13083-970 Campinas, SP, Brazil. Tel.: +55 19 3521 3023.
E-mail address: zezzi@iqm.unicamp.br (M.A.Z. Arruda).

0039-9140/$ - see front matter © 2013 Elsevier B.V. All rights reserved.
http://dx.doi.org/10.1016/j.talanta.2013.09.030

source was, also used, and the operating conditions were those recommended by the manufacturer (λ=286.3 nm and 0.7 nm spectral band pass). All measurements were based on integrated absorbance in triplicate.

The on-line hydride generation system was employed according to Klassen et al. [5], which comprised a peristaltic pump (Ismaltec IPC) and a polymethacrylate three-piece injector-commutator and gas–liquid separator device designed and build-up in our laboratories. Polyethylene tubes (0.7 mm i.d.), as transmission lines, and Tygon® tubes for propelling the solutions were used. A Provecto Analítica microwave oven, model DGT Plus (Jundiaí, Brazil), was used for sample decomposition.

2.2. Reagents and solutions

All solutions were prepared using analytical reagent grade as well as high purity deionizer water (18.2 MΩ cm) from a Millipore model Milli-Q Plus water purification unit. All glasswares were washed with soap and kept in 10% (v/v) HNO_3 for 24 h with subsequent cleaning with deionizer water. Reference solution of Sn was prepared daily using 0.2 mol L^{-1} HNO_3 by serial dilution from standard stock solutions containing 1000 mg L^{-1} (Tec-Lab, Jundiaí, São Paulo, Brazil) in deionized water. Solution of sodium tetrahydroborate (−1) (THB) (Sigma Aldrich, Steinheim, Germany) 0.2 mol L^{-1} was also prepared daily in 0.1 mol L^{-1} NaOH (Merck, Darmstadt, Germany) for Sn determination.

2.3. Hydride generator and metallic furnace atomizer

A hydride generation metallic furnace atomic absorption spectrometry (HG-MF-AAS) system (Fig. 1) was mounted with metallic furnace atomizer (Inconel600® tube atomizer, Camacam, São Paulo, Brazil) and based on Klassen et al. [5] and Figueiredo et al. [6]. The metal atomizer was positioned on the burner of FAAS. Then, a ceramic capillary was connected to the atomizer, in order to allow the introduction of the hydrides from the Flow Injection Analysis (FIA) system.

In this system, the acidified sample and THB are aspirated by a peristaltic pump, filling the loops. After injecting both solutions through an injector-commutator, they are mixed in the confluence point, and the reaction taking place in the reaction coil, which ensures the required time for the hydride formation. Then, the hydride is separated from the liquid phase in the gas–liquid separator, and transported by the carrier gas (argon) towards to FAAS. In this way, the hydride pass through the ceramic capillary, being then introduced into the metallic furnace atomizer. The tube positioned on the burner has six holes in the face addressed to the burner, allowing the partial flame penetration inside of the tube, and promoting the Sn atomization.

2.4. Samples

Accuracy and precision of the HG-MF-AAS method were evaluated using two standard reference materials: PACS-2 (Marine Sediment Reference Materials for Trace Metals and other Constituents, National Research Council of Canada, NRC-CNRC) and NIST SRM 1643e (Trace Element in Water).

For the sediment, 0.200 mg (n=3) were weighted in a Teflon® flask, and tin, at three different levels, was added for which the final concentrations were 125, 250 and 375 μg L^{-1}. A blank (n=3) was also performed. Then, 5 mL conc. HNO_3 and 0.5 mL of 30% (v/v) H_2O_2 were added. All samples were submitted to the microwave oven program as observed in Table 1.

After this procedure, the samples were filtered and brought to near dryness for reducing the acidity, and the volume completed to 25 mL. Tin was the determined by the HG-MF-AAS method in the optimized conditions.

For water, to each 2.5 mL, three tin levels were added, obtaining the final concentration of 125, 250 and 375 μg L^{-1}. Then, the solution was completed to 10 mL. A blank was also performed. Tin was then determined by the HG-MF-AAS method in the optimized conditions. Additionally, the sample without standard addition was considered as blank (n=3).

2.5. Concomitant evaluation

Some concomitants were evaluated for verifying if they interfere in the tin determination by HG-MF-AAS. Copper, lead and zinc at the 1:1, 1:10 and 1:20 (Sn:concomitant) ratios were, respectively, evaluated, considering a tin concentration of 250 μg L^{-1}.

2.6. The metallic furnace morphology by SEM

After all experiments, the Inconel600® tube atomizer morphology was evaluated by Scanning Electron Microscopy (SEM). For that, the metallic furnace employed in this work was cut in three parts (two at each extremity and one at the center of the tube). Then, in the SEM's carbon stubs, the material was fixed in a carbon tape and the scanning electron microscope for surface image obtaining was the taken, as well as some elements distribution in the atomizer according to the follow conditions: accuracy

Table 1
Program used for sediment sample decomposition.

Step	Time (min)	Power (W)
1	3	200
2	5	400
3	5	600
4	20	700
5	2	80

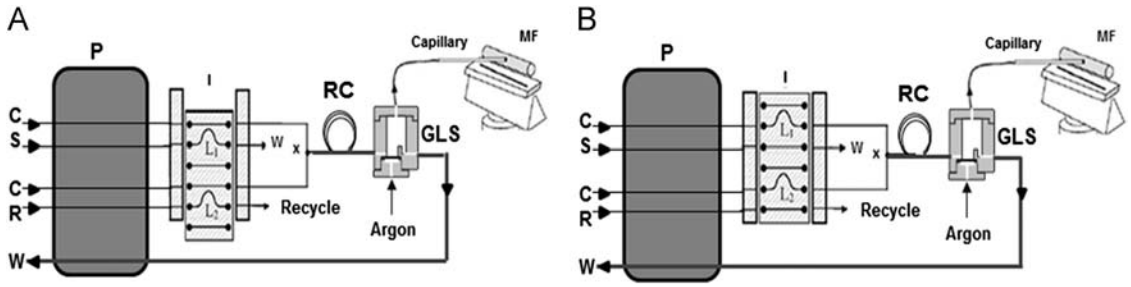

Fig. 1. Schematic diagram of the flow injection system proposed. [P]: peristaltic pump; [I]: injector–commuter; [x]: confluence point; [RC]: reaction coil; [GLS]: gas–liquid separator; ceramic capillary and Inconel600® metallic furnace (MF); [C] carrier solution (deionized water); [S] standards/samples (in acidic media); [R] THB in NaOH; and [W] waste. (A) System in the sampling position. [L1]: Sample; [L2]: THB in NaOH. (B) System in injection position[5].

voltage of 20 kV, resolution of 512 × 384 pixels, acquisition time of 102 s and dwell time of 27 s.

3. Results and discussion

3.1. Chemical variables optimization

All optimizations were carried out with a Inconel600® tube atomizer, and 500 μg L^{-1} of Sn reference solution. After optimizing each condition, a calibration curve was obtained for checking the sensitivity of the method.

The type and concentration of the carrier were the two first variables optimized. Acidity is an important parameter in the hydride generation process, because it is necessary for activating the borane complexes in order to produce the intermediaries, and, subsequently, allow the generation of hydride [1]. Then, nitric and hydrochloric acids were tested at 0.20 mol L^{-1} as well air as carriers.

Through the results, nitric acid besides the best tin integrated absorbance (0.32 ± 0.03) by comparing with HCl (0.25 ± 0.03) and air (0.17 ± 0.04), also presented the best signal profile (date not show). The tin and NaOH concentrations in this case were 500 μg L^{-1} and 0.10 mol L^{-1}, respectively. As nitric acid was choosen as carrier, its concentration was tested from 0.01 to 2.0 mol L^{-1}. The detectability increased from 0.01 to 0.2 mol L^{-1} (from 0.02 to 0.32 A s) and linearly decreased after this concentration (see Fig. 2). According to Pitzalis et al. [8], a decrease on the efficiency of stannane generation at low acidity due the loss of substrates or due to the insoluble species formation is usually observed [8], once the low efficiency in hydride generation at higher acidity can be explained by the lack of reactivity between the analysis substrates and THB species [1]. According to D'Ulivo et al., the optimum acidity for stannane generation is shown in the small range concentration between 0.1 and 0.2 mol L^{-1}, which corroborates with our results [1].

Another important parameter in hydride generation is the NaOH concentration, once that, it prevents the hydrolysis of the reducing agent (THB) [1,9]. Its concentration was ranged from 0.01 to 1.00 mol L^{-1}. Although 0.50 mol L^{-1} NaOH concentration shows a little increase in the integrated absorbance (ca. 15%), it a worst signal profile by comparing with 0.10 mol L^{-1} concentration. Additionally, 0.10 mol L^{-1} concentration shows the lowest standard deviation (2.52% RSD) and this value was considered as work condition.

The last parameter tested was the influence of THB concentration. The THB is the reducing agent mostly employed in hydride generation mainly due to the fast formation of hydride and possibility of employing an automated system such as flow injection [9]. Thus, concentrations of THB between 0.02 and 0.50 mol L^{-1} were evaluated. According to the results, a higher integrated absorbance (0.34 ± 0.02) was observed by increasing the THB concentration until 0.20 mol L^{-1}. From this concentration, no increase on the integrated absorbance is observed. This behavior is due to a higher efficiency on the hydride generation with the increase in THB concentration. However, from 0.5 mol L^{-1} THB concentration, there was an increase in hydrogen formation [6], which does not contribute for the increase in integrated absorbance. Thus, 0.20 mol L^{-1} THB was fixed for future experiments.

3.2. Physical variables optimization

The first physical variable evaluated was the carrier flow-rate, which was ranged from 1 to 8 mL min^{-1}. It is observed that an increase in integrated absorbance of ca. 10% by comparing 1 and 2 mL min^{-1}. From this flow-rate no statistical difference was observed, the optimized value being 2 mL min^{-1}.

The proportion of acetylene and air in the flame was observed as next step. The acetylene and air flow-rate were varied between 1 to 4 and 8 to 12 L min^{-1}, respectively. Through Fig. 3, one can note that 1 and 9 L min^{-1} acetylene and air flow-rate, respectively, showed higher integrated absorbance for each condition evaluated. However, considering other conditions a high memory effect was observed, which was checked through the blank signal profile obtained after injecting the tin standard solution. Then, the proportion of

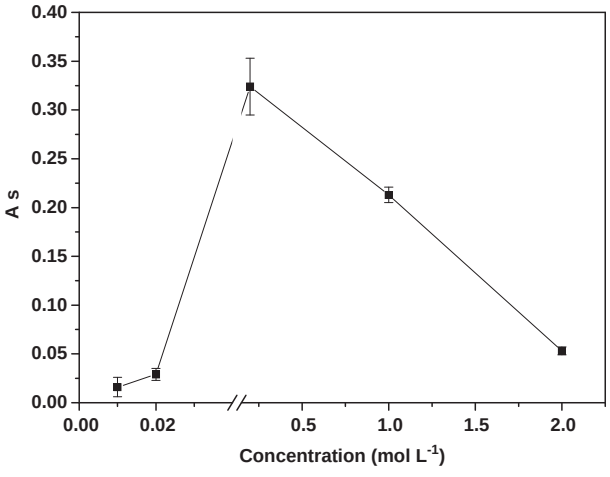

Fig. 2. Optimization of nitric acid concentration. Conditions employed: 500 μg L^{-1} of Sn, 0.20 mol L^{-1} of THB and 0.10 mol L^{-1} of NaOH.

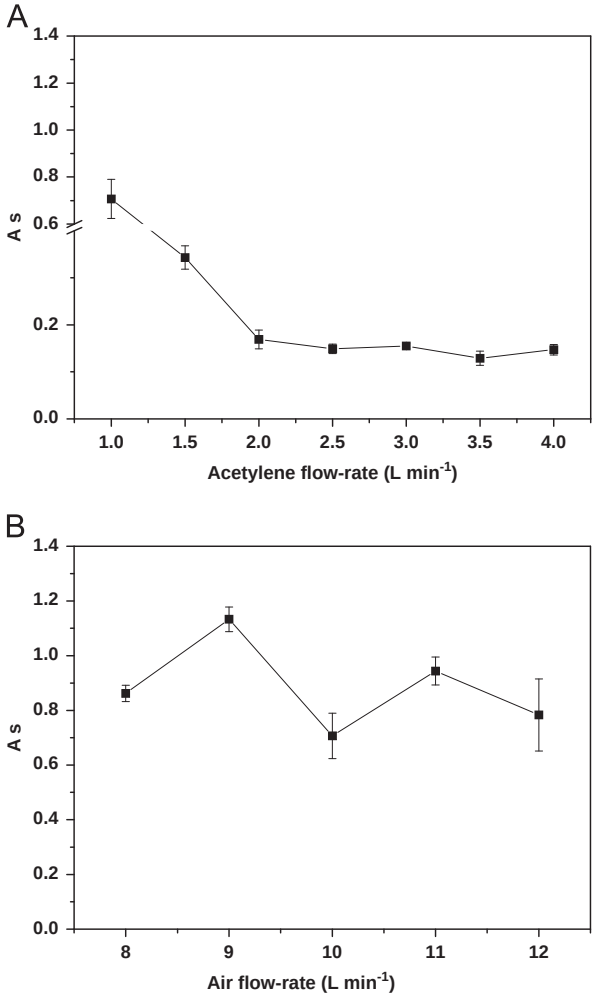

Fig. 3. Influence of acetylene (A) and air (B) flow-rate in the flame. Conditions employed: 500 μg L^{-1} of Sn, 0.20 mol L^{-1} of THB and 0.20 mol L^{-1} HNO_3.

1.5:10 L min^{-1} of acetylene and air was respectively employed, once that at this condition, no memory effect was verified.

For the next optimization the injected volumes of sample and reducing agent between 250 and 1500 μL were evaluated. Although linear increment of ca. 13 times was observed in the integrated absorbance when 1500 μL was used, the volume of 1000 μL was fixed for the next steps because better peak shapes were obtained.

After defining the injected volume, the argon flow-rate in the gas–liquid separator between 50 and 350 mL min^{-1} was evaluated, once that it transports the hydride into the metallic atomizer. An increase of argon flow-rate confers an increase on the integrated absorbance (ca. 255%) until 300 mL min^{-1}, and from this value only slight one. Then, 300 mL min^{-1} was fixed, showing good efficiency on the hydride transport.

The next step was then the optimization of the length of the reactor coil, which was tested between 30 and 150 cm. This is an important parameter, once that the conversion of the analyte into hydrides is kinetic-dependent. From Fig. 4, one can observe the dependency of the detectability and the coil length, once that the stannane presents a slow kinetic of formation. Then, using a coil of 120 cm, an increment of ca. 16% on the detectability was obtained, making this length fixed for further experiments.

The use of deionized water in the nebulizer of the FAAS equipment when working with the HG-MF-AAS system is recommended to avoid the superheating of this system. Then, the water flow-rate in the nebulizer between 1 and 5 mL min^{-1} was evaluated. The flow-rate of 1 mL min^{-1} was then fixed, because the highest integrated absorbance was attained.

Finally, the influence of Inconel600® total hole area between 0 and 67 mm^2 was evaluated. These areas represent the sum of each six holes in the bottom of the tube atomizer. For 19 mm^2 total hole area, a great increase in the integrated absorbance compared with the atomizer without hole was attained. This increase of the signal with a partial entrance of the oxidant flame in the atomizer, suggests the tin route atomization through the oxides formation [10]. For higher hole areas than 19 mm^2, a decrease in the integrated absorbance was verified. Most probably, the excess of oxygen can react with the analyte, thus forming oxides which are hard to be decomposed [11]. Then, a 19 mm^2 total hole area in metallic furnace atomizer was fixed for next tests.

Before the sample analysis, a test with a 1250 μL injected volume of THB was carried out to assure that all tin solution could react with the reducer. This increase in the volume injected of THB provided an increase in the integrated absorbance (ca. 23%), showing that at previous conditions, good mixing between tin solution and THB was attained.

After the optimization of each parameter for tin determination, the optimized conditions can be observed in Table 2.

At these final conditions, the HG-MF-AAS method presented a linear Sn concentration from 50 to 1000 μg L^{-1} ($r > 0.9995$; $n=3$) and an analytical frequency of ca. 40 h^{-1}. The limit of detection (LOD) and quantification (LOQ) were 7.1 and 23.7 μg L^{-1}, respectively, and were estimated based on the IUPAC definitions [12]. Finally, the precision, expressed as RSD, was less than 4% (200 μg L^{-1}; $n=10$).

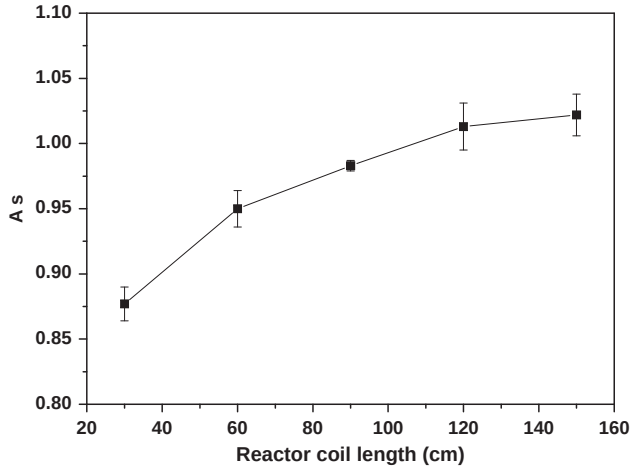

Fig. 4. Influence of reactor coil length. Conditions employed: 500 μg L^{-1} of Sn, 0.20 mol L^{-1} of HNO_3, 0.20 mol L^{-1} of THB and 0.10 mol L^{-1} of NaOH.

3.3. Concomitant evaluation

Table 3 shows the results, pointing out the interferences occurring only with copper at 1:10 and 1:20 ratios, with a significant reduction of the analytical signal. This fact can be explained either by its reaction with the reducing agent or due to the consumption of the analyte in the solution, producing a decrease on the sensitivity [1].

3.4. Accuracy purpose

After all optimization and concomitant evaluation, the accuracy and precision of the proposed method were then evaluated using two standard reference materials (PACS-2 – sediment and SRM 1643e – water sample). The results can be observed through Table 4, and good recoveries were attained.

Table 2
Optimized conditions for the determination of tin by HG-MF-AAS.

Variables	Optimized condition
Chemical	
Type of carrier	HNO_3
Concentration of carrier	0.2 mol L^{-1}
Concentration of NaOH	0.1 mol L^{-1}
Concentration of THB	0.2 mol L^{-1}
Physical	
Carrier flow-rate	4 mL min^{-1}
Acetylene flow-rate	1.5 L min^{-1}
Air flow-rate	10 L min^{-1}
Injected volume of Sn	1000 μL
Injected volume of THB	1250 μL
Argon gas flow-rate	300 mL min^{-1}
Reactor coil length	120 cm
Water flow-rate in the nebulizer	1 mL min^{-1}
Inconel600® tube total hole area	19 mm^2

Table 3
Evaluation of concomitants for the determination of tin by HG-MF-AAS.

Concomitant	Sn (250 μg L^{-1}): concomitant ratio	Recovery (%)
Cu	1:1	98 ± 3
	1:10	63 ± 5
	1:20	50 ± 2
Pb	1:1	94 ± 2
	1:10	99 ± 2
	1:20	101 ± 2
Zn	1:1	91 ± 3
	1:10	91 ± 2
	1:20	95 ± 1

3.5. Atomizer morphology analysis by SEM

The evaluation of the Inconel600® tube atomizer was carried out by SEM, as demonstrated in Fig. 5, where one can note the different parts analyzed (1–3). This strategy was adopted taken into account those morphologic modifications observed in previous work published by our research group, but considering stibine, bismutine, and selenium hydride for Sb, Bi and Se determinations, respectively [5,6]. When considering a new tube (Fig. 6), a smooth surface was observed, with a homogeneous distribution of the main constituents of Inconel600® alloy (nickel, chromium and iron).

By comparing a new (Fig. 6) and used (after 150 h) tube atomizer (Fig. 7), one can see that the main constituents of the Inconel600® alloy remained homogeneously distributed in the atomizer, suggesting that such elements do not effectively participate in the tin atomization route.

Furthermore, through the results obtained for the main elements distribution in the inner surface of the metallic furnace employed in this work, other important fact, discussed in Section 3.2, related to the tin atomization route can be confirmed, once great amount of oxides are present in atomizer surface after finishing the experiments. These oxides are homogeneously distributed for all over inner surface of metallic furnace while that, for the new tube, the presence of these oxides in its surface was not observed. Therefore, considering the oxidant flame employed, as well as the SEM images, there are evidences that the tin atomization route actually occurs through oxide formation.

Table 4
Recovery for tin in sediment (PACS-2) and water (1643e) samples.

Material	Sn expected concentration	Sn concentration determinated	Recovery (%)[a]
PACS-2	125 μg kg^{-1}	153 ± 19 μg kg^{-1}	121 ± 13
	250 μg kg^{-1}	242 ± 2 μg kg^{-1}	95 ± 1
	375 μg kg^{-1}	289 ± 7 μg kg^{-1}	76 ± 2
1643e	125 μg L^{-1}	129 ± 8 μg L^{-1}	101 ± 2
	250 μg L^{-1}	257 ± 14 μg L^{-1}	102 ± 4
	375 μg L^{-1}	394 ± 6 μg L^{-1}	104 ± 2

[a] For all experiments, $n=3$.

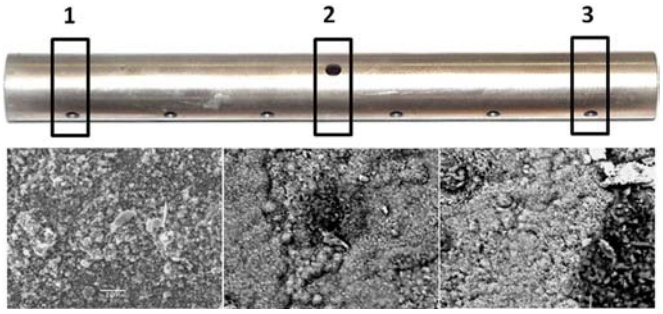

Fig. 5. Image of over inner surface of the Inconel600® atomizer employed in this work by SEM. Increase by 1500 times.

4. Conclusions

The initial purpose of this work was successfully attained, making possible the tin determination in different samples, such as water and river sediment. To the best of our knowledge, this is the first work in the literature regarding Sn determination using hydride generation with metallic atomizers.

While the nitric acid presented the best signal profile for tin, being then elected as carrier to the flow system, the main important physical parameter was the hole area of the metallic tube, because its size influences the formation of the refractory tin species or allows a good tin atomization. Then, 19 mm^2 total hole area was

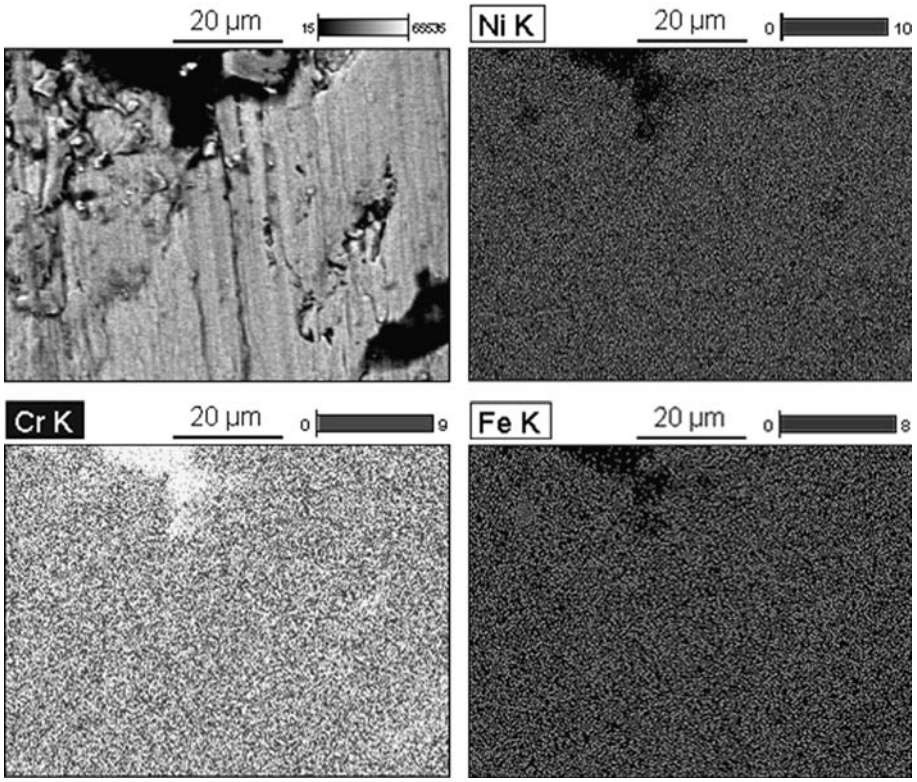

Fig. 6. Image and principal elements distribution for over inner surface of a new Inconel600® atomizer by SEM. Increase by 1500 times.

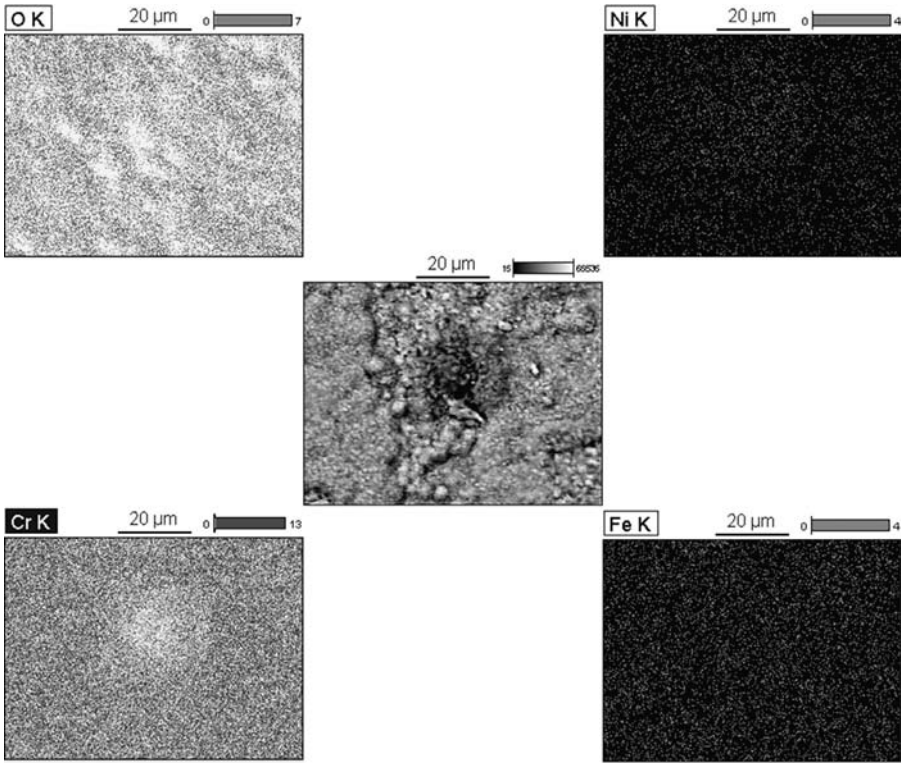

Fig. 7. Image and main elements distribution for over inner surface of an Inconel600® atomizer employed in this work by SEM. Increase by 1500 times.

chosen in this work. Another important conclusion after analyzing the scanning electron micrography images was that the elements present in the alloy do not participate in the atomization of tin, once that they were homogeneously distributed onto the inner surface of the metallic atomizer.

Another important point always emphasized is the low cost implementation of such systems, once that each metallic tube costs ca. US$ 7 and its durability is more than 2000 h. The ceramic capillary also costs ca. US$ 5 and its durability is 10 times more than the own tube.

Acknowledgments

The authors thank the Fundação de Amparo a Pesquisa do Estado de São Paulo (FAPESP, São Paulo, Brazil) for financial as well as the Conselho Nacional de Desenvolvimento Científico e Tecnológico (CNPq, Brasília, Brasil) for a fellowship to M.A.Z.A and to Coordenação de Aperfeiçoamento de Pessoal de Nível Superior (CAPES, Brasília, Brasil) for financial assistance.

References

[1] A. D'Ulivo, J. Dědina, Z. Mester, R.E. Sturgeon, Q. Wang, B. Welz, Pure Appl. Chem. 83 (2011) 1283–1340.
[2] A. Gáspár, H. Berndt, Spectrochim. Acta B 55 (2000) 587–597.
[3] J. Dědina, T. Matousek, J. Anal. At. Spectrom. 15 (2000) 301–304.
[4] A. Klassen, E.C. Figueiredo, N. Baccan, M.A.Z. Arruda, Br. J. Anal. Chem. 1 (2010) 110–114.
[5] A. Klassen, M.L. Kim, M.B. Tudino, N. Baccan, M.A.Z. Arruda, Spectrochim. Acta B 63 (2008) 850–855.
[6] E.C. Figueiredo, J. Dědina, M.A.Z. Arruda, Talanta 73 (2007) 621–628.
[7] E.L. Lehmann, A.H. Fostier, M.A.Z. Arruda, Talanta 104 (2013) 187–192.
[8] E. Pitzalis, M.C. Mascherpa, M. Onor, A. D'Ulivo, Spectrochim. Acta B 64 (2009) 309–314.
[9] J. Dědina, D.L. Tsalev, Hydride Generation Atomic Absorption Spectrometry, first ed., John Wiley & Sons, Chichester, 1995.
[10] B. Welz, M. Sperling, Atomic Absorption Spectrometry, third ed., John Wiley & Sons, Weinheim, 1999.
[11] H. Matusiewicz, M. Krawczyk, Anal. Lett. 43 (2010) 2543–2562.
[12] J. Inczédy, T. Lengyel, A.M. Ure, in: J. Inczédy, T. Lengyel, A.M. Ure (Eds.), Compendium of Analytical Nomenclature: Definitive Rules 1997, third. ed., IUPAC—International Union of Pure and Applied Chemistry Division, 1997.